nature structural & molecular biology

The structural basis of transferrin sequestration by transferrin-binding protein B

Charles Calmettes[1], Joenel Alcantara[2,3], Rong-Hua Yu[2,3], Anthony B Schryvers[2,3] & Trevor F Moraes[1]

***Neisseria meningitidis*, the causative agent of bacterial meningitis, acquires the essential element iron from the host glycoprotein transferrin during infection through a surface transferrin receptor system composed of proteins TbpA and TbpB. Here we present the crystal structures of TbpB from *N. meningitidis* in its apo form and in complex with human transferrin. The structure reveals how TbpB sequesters and initiates iron release from human transferrin.**

N. meningitidis and *N. gonorrhoeae* are globally prevalent causes of bacterial meningitis and gonorrhea, respectively. In order to colonize and infect its host, *Neisseriaceae*, *Pasteurellaceae* and *Moraxellaceae* pathogens have an iron-uptake system that is based on the transferrin-binding proteins TbpA and TbpB, which together function to extract iron from transferrin[1]. TbpA is a 100-kDa TonB-dependent outer-membrane protein essential for iron uptake, which has been proposed to serve as a channel for iron transport across the outer membrane[2]. TbpB is a bilobed 60- to 80-kDa lipid-anchored protein that is essential for host colonization[3] and that extends from the outer membrane into the host milieu in order to bind and sequester transferrin in the first step of iron acquisition[4]. Both TbpA and TbpB bind to the transferrin C-lobe[5]. TbpB specifically recognizes the iron-loaded form of transferrin, whereas TbpA indiscriminately binds the holo or apo form of transferrin[6]. Hence, it has been proposed that TbpB recruits iron more efficiently from iron-saturated transferrin *in vivo*. TbpB has been explored for vaccine development owing to its essential iron-recruiting function and because it can induce a protective immune response against a variety of different pathogenic bacteria[7,8].

To determine the molecular events during iron uptake by TbpB, we have determined the X-ray crystal structures of the TbpB receptor from *N. meningitidis* strain M982 (*Nm*M982) in its apo form (at 2.15 Å resolution) and in complex with human transferrin (at 2.95 Å resolution) (**Fig. 1a**, **Supplementary Table 1** and **Supplementary Fig. 1**). Similar to the previously characterized TbpB from porcine pathogens (*Actinobacillus pleuropneumoniae* and *A. suis*)[4,9], *Nm*M982-TbpB is a bilobed protein with each lobe subdivided into a β-barrel domain and an adjacent handle domain (**Fig. 1a**).

Within the TbpB–human transferrin complex, human transferrin also appears as a bilobed protein with ferric iron (Fe^{3+}) binding sites within each of the N- and C-lobes[10]; one iron element can be visualized within the C-lobe iron-binding site while the N-lobe site is in the apo form (**Fig. 1a**). Each of the human transferrin lobes are divided in two subdomains connected by a hinge that is at the base of a deep cleft containing the iron-binding site. The iron-free N-lobe aligns structurally with the open N-lobe from the apo human transferrin (PDB 2HAU) previously characterized[11] (r.m.s. deviation = 0.65 Å). The TbpB–human transferrin structure describes the first human iron-coordinated C-lobe. The C-lobe contains a hexacoordinated Fe^{3+} bound to four highly conserved amino acid residues in the C1 and C2 domains: Asp392, Tyr426, Tyr517 and His585 (**Supplementary Fig. 2a–c**). The final two iron-coordinating groups are provided by a carbonate ion, similarly to diferric rabbit and porcine transferrins (PDB 1JNF and 1H76)[10]. The carbonate is stabilized by hydrogen bonds with Thr452, Arg456 and the peptide backbone amide of Ala458. Superposition of the monoferric human transferrin C-lobe with the diferric rabbit and porcine transferrins[10] reveals that there is structural conservation of these C-lobe structures (r.m.s. deviation = 0.55 Å and 0.51 Å, respectively) within the closed (holo) conformation.

The TbpB–human transferrin complex is held together by extensive interactions between the TbpB N-lobe and the holo human transferrin C-lobe. The heterodimer complex buries a substantial surface area of ~1,450 $Å^2$, in which the C1 and C2 human transferrin subdomains dock onto the TbpB N-lobe handle and β-barrel domains, respectively (**Fig. 1**). The TbpB–human transferrin structure is in good agreement with our predicted model created from hydrogen-deuterium exchange MS experiments and targeted TbpB–transferrin mutant characterizations (**Fig. 1b**)[4,9,12,13]. In addition, we have validated the interface of the complex structure through binding assays with wild type and mutants (R199A and E222R) of *Nm*M982-TbpB; insertion of a charge reversal within the buried interface leads to a drastic loss of binding capacity (**Fig. 1c**). The large binding interface between TbpB and human transferrin involves 16 hydrogen bonds, 4 salt bridges, 6 bridging waters, and hydrophobic interactions, along the entire cap area of the TbpB N-lobe (amino acid contacts are listed in **Supplementary Table 2**), which function to stabilize the human transferrin C-lobe that is iron-loaded onto TbpB.

Previous works have shown that the N- and C-lobes of transferrin contain pH-sensitive residues that monitor the conformational changes of transferrin: the dilysine motif[14] Lys206-Lys296 in the N-lobe, and the Lys534-Arg632-Asp634 triad[15] and the His349-Lys511 motif[16] within the C-lobe. Within the TbpB–human transferrin structure, the His349-Lys511 motif in human transferrin is buried in the binding interface, and the His349 residue interacts with TbpB

[1]Department of Biochemistry, University of Toronto, Toronto, Ontario, Canada. [2]Department of Microbiology & Infectious Diseases, University of Calgary, Calgary, Alberta, Canada. [3]Department of Biochemistry & Molecular Biology, University of Calgary, Calgary, Alberta, Canada. Correspondence should be addressed to T.F.M. (trevor.moraes@utoronto.ca).

Received 9 November 2011; accepted 19 January 2012; published online 19 February 2012; doi:10.1038/nsmb.2251

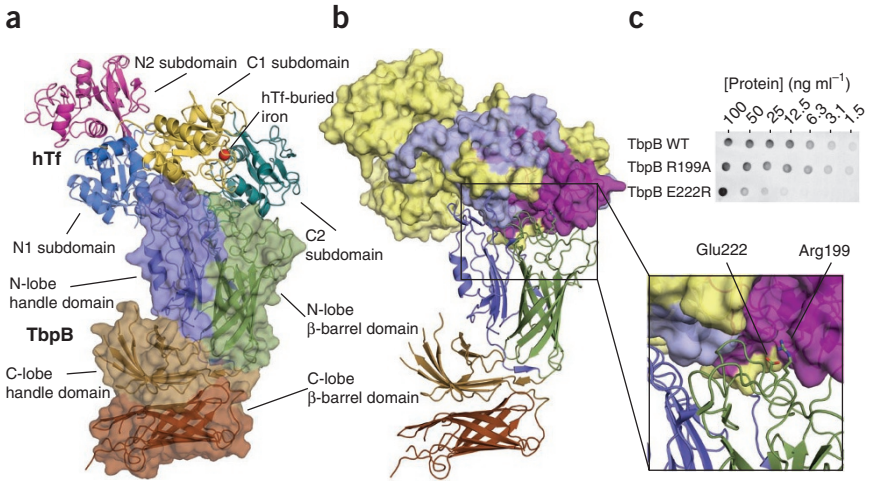

Figure 1 The structure of the *Nm*M982-TbpB–human transferrin complex. (**a**) Cartoon representation of TbpB in complex with human transferrin (hTf) from residues 3 to 679. TbpB (residues 38–691) is shown as a space-filled diagram, and human transferrin is shown in ribbon representation; domains and subdomains from both proteins are shown in different colors and are labeled. (**b**) Cartoon of TbpB in ribbon representation with subdomains colored as in **a**. The surface of human transferrin is colored on the basis of previous hydrogen-deuterium exchange mapping[12]. Purple denotes areas protected in the presence of TbpB, yellow denotes unprotected regions and gray denotes sequences for which no peptide was detected by MS analysis. (**c**) Interaction of *Nm*M982-TbpB (wild type and mutants) with human transferrin, as assessed by binding assays on nitrocellulose membrane and anti-human transferrin antibody (see **Supplementary Methods** for details).

through a tetrahedrally coordinated bridging water that forms hydrogen bonds with Asp159, His143, Lys206 from TbpB and His349 from human transferrin (**Fig. 2** and **Supplementary Fig. 2d–h**). The human transferrin His349 residue has been shown to have a crucial role in the pH-inducible switch response for iron release in the presence of the human transferrin receptor (TfR)[16,17]. Protonation of His349 on the C1 subdomain is proposed to induce electropositive repulsion of the opposite facing residue Lys511 on the C2 subdomain, leading to conformation changes and resulting in the opening of transferrin in low pH conditions[16,17]. Within the described structured water pocket, His143 (from TbpB) and the minor His349 conformation are in close proximity to the Lys511 that could elicit charge repulsion between the C1 and C2 subdomains, depending on their protonated state. A structure-based pK_a prediction, using PROPKA[18], suggests that TbpB stabilizes the holo C-lobe conformation by reducing the estimated pK_a of human transferrin His349 from 6.2 in the unbound form to 1.9 in the TbpB-bound form (**Fig. 2b**). We propose that the human transferrin–TbpB interface prevents His349 from becoming protonated and stabilizes the iron-loaded C-lobe of human transferrin.

Transferrin-bound and unbound TbpBs have an almost identical main chain and loop organization in the human transferrin–binding site, except that the peripheral loop $L_{102–124}$ shifts outward to allow the human transferrin loop $L_{496–515}$ to dock onto TbpB. The binding does not generate any major structural changes within TbpB (r.m.s. deviation = 0.4 Å between the bound and unbound N-lobe; see **Supplementary Fig. 1b**). The TbpB–human transferrin recognition acts similarly to a rigid body docking between the two proteins. The only feature differentiating the human transferrin-bound TbpB from the unbound TbpB is a torsion rotation of 5.4° into the orthogonal lattice between the TbpB N- and C-lobes, which could be a consequence of the crystal contacts (**Supplementary Fig. 3**).

The bacterial TbpB receptor competes for transferrin with the mammalian TfR that is located on the surface of host cells and mediates iron release from transferrin in a pH-dependent mechanism driven by the acidification of the endosome. The TfR-binding site on transferrin has been described on both the N- and C-lobe domains of transferrin[17], whereas the bacterial receptor TbpB binds uniquely to the C-lobe domain of transferrin. The TbpB-binding site on human transferrin partially overlaps with the TfR-binding interface, sharing helix 1 as a common interaction site (**Supplementary Fig. 4**). This overlapping binding site on human transferrin for host and invading *Neisseriaceae*, *Pasteurellaceae* or *Moraxellaceae* pathogens allows the bacteria to circumvent mutations on transferrin, which thus provide no advantage to the host in terms of iron sequestration from transferrin, as both TfR and TbpB directly compete for a similar surface on human transferrin.

The mammalian TfR has no retrieving specificity, whereas the bacterial receptor TbpB binds uniquely to the holo transferrin of its host species[19], despite the high sequence conservation among serotransferrins. Distinctly from TfR, TbpB interacts with the loop $L_{496–515}$ of human transferrin, which is a region of diverse length and sequence in mammalian homologs of transferrin (**Supplementary Fig. 4e**); superposition of human transferrin with porcine transferrin illustrates that steric hindrance between porcine $L_{496–515}$ and *Nm*M982-TbpB would prevent *Nm*M982-TbpB from forming a complex with porcine transferrin. These variations of the transferrin loop $L_{496–515}$ within the TbpB-recognition site seem to address a major barrier for cross-species specificity between the TbpB pathogen receptors and transferrin homologs. Furthermore, the TbpB–human transferrin complex structure provides a structural explanation of the TbpB specificity for the holo form of the transferrin C-lobe, as both the C1 and C2 subdomains dock onto TbpB, whereas the open conformation is characterized by a 51° rotation of the C2 domain, which would drastically reduce the binding interface between TbpB and transferrin.

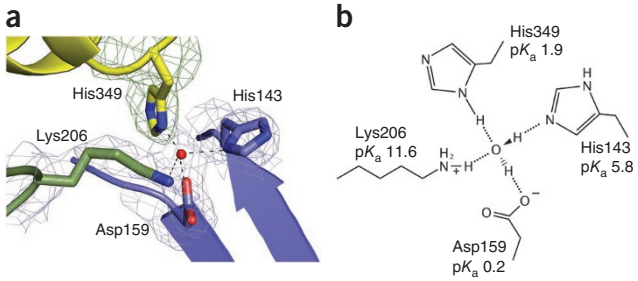

Figure 2 TbpB stabilizes the holo form of human transferrin. (**a**) The cartoon representation of the buried His349 from human transferrin in contact with His143, Asp159 and Lys206 from TbpB illustrates the interaction of these residues through a tetrahedrally coordinated bridging water within the binding interface. The four residues and the tetrahedrally coordinated water (red sphere) are embedded within a simulated annealing $2F_o - F_c$ electron density map at 1.0 σ, without the human transferrin His349 residue. Yellow, green and blue denote the C1 human transferrin domain, the TbpB N-lobe β-barrel domain and the handle domain, respectively. (**b**) The schematic model of the tetrahedrally coordinated water is shown with the structure-based predicted pK_a values for each residue indicated.

The structural data presented here provide the basis for transferrin–TbpB recognition, an essential function for the survival of many host-restricted pathogens, including *N. meningitidis*, in the iron-limited environment of the host blood[20]. Our data reveal that TbpB does not initiate the opening of the human transferrin holo C-lobe that leads to iron release. Instead, as the X-ray crystal structure of TbpB–human transferrin demonstrates, TbpB buries the critical human transferrin residue His349 in a controlled environment that leads to stabilization of the human transferrin C-lobe holo form. This is consistent with TbpB recruiting and sequestering iron-loaded transferrin while inside the host and maintaining the iron-loaded status of transferrin until its delivery to TbpA. This structural insight into the function of TbpB–human transferrin during the first step of the iron-acquisition process suggests that the second step of the iron-acquisition mechanism consists of TbpA or the ternary complex human transferrin–TbpA–TbpB initiating conformational changes within transferrin to release iron.

Accession codes. Structure factors and atomic coordinates for *Nm*M982-TbpB and the *Nm*M982-TbpB–human transferrin complex have been deposited with accession codes 3VE2 and 3VE1, respectively.

Note: Supplementary information is available on the Nature Structural & Molecular Biology website.

ACKNOWLEDGMENTS

We thank members of the Advanced Photon Source at both of the Northeastern Collaborative Access Team's beamlines 24-ID-E and 24-ID-C, the Canadian Light Source beamline staff at the Canadian Macromolecular Crystallography Facility CMCF-08ID-1 for assistance with data collection, and members of the Moraes and Schryvers laboratories for valuable discussions. This research was funded with operating and infrastructure support provided by the Canadian Foundation for Innovation, the Alberta Innovates Health Solutions and the Canadian Institutes of Health Research.

AUTHOR CONTRIBUTIONS

C.C., A.B.S. and T.F.M. conceived and designed the experiments, C.C. conducted experiments and data analysis, J.A. provided the wild-type *Nm*M982-TbpB–containing plasmid, R.-H.Y. provided deglycosylated human transferrin and C.C. and T.F.M. wrote the manuscript. All authors read and commented on the draft versions of the manuscript and approved the final version.

COMPETING FINANCIAL INTERESTS

The authors declare no competing financial interests.

Published online at http://www.nature.com/nsmb/.
Reprints and permissions information is available online at http://www.nature.com/reprints/index.html.

1. Gray-Owen, S.D. & Schryvers, A.B. *Trends Microbiol.* **4**, 185–191 (1996).
2. Cornelissen, C.N. *et al. Mol. Microbiol.* **27**, 611–616 (1998).
3. Baltes, N., Hennig-Pauka, I. & Gerlach, G.F. *FEMS Microbiol. Lett.* **209**, 283–287 (2002).
4. Moraes, T.F., Yu, R.H., Strynadka, N.C. & Schryvers, A.B. *Mol. Cell* **35**, 523–533 (2009).
5. Alcantara, J., Yu, R.H. & Schryvers, A.B. *Mol. Microbiol.* **8**, 1135–1143 (1993).
6. Retzer, M.D., Yu, R., Zhang, Y., Gonzalez, G.C. & Schryvers, A.B. *Microb. Pathog.* **25**, 175–180 (1998).
7. Danve, B. *et al. Vaccine* **11**, 1214–1220 (1993).
8. Myers, L.E. *et al. Infect. Immun.* **66**, 4183–4192 (1998).
9. Calmettes, C. *et al. J. Biol. Chem.* **286**, 12683–12692 (2011).
10. Hall, D.R. *et al. Acta Crystallogr. D Biol. Crystallogr.* **58**, 70–80 (2002).
11. Wally, J. *et al. J. Biol. Chem.* **281**, 24934–24944 (2006).
12. Ling, J.M., Shima, C.H., Schriemer, D.C. & Schryvers, A.B. *Mol. Microbiol.* **77**, 1301–1314 (2010).
13. Silva, L.P. *et al. J. Biol. Chem.* **286**, 21353–21360 (2011).
14. Steinlein, L.M., Ligman, C.M., Kessler, S. & Ikeda, R.A. *Biochemistry* **37**, 13696–13703 (1998).
15. Halbrooks, P.J. *et al. Biochemistry* **42**, 3701–3707 (2003).
16. Steere, A.N. *et al. J. Biol. Inorg. Chem.* **15**, 1341–1352 (2010).
17. Eckenroth, B.E., Steere, A.N., Chasteen, N.D., Everse, S.J. & Mason, A.B. *Proc. Natl. Acad. Sci. USA* **108**, 13089–13094 (2011).
18. Li, H., Robertson, A.D. & Jensen, J.H. *Proteins* **61**, 704–721 (2005).
19. Schryvers, A.B. & Gonzalez, G.C. *Can. J. Microbiol.* **36**, 145–147 (1990).
20. Echenique-Rivera, H. *et al. PLoS Pathog.* **7**, e1002027 (2011).